



Published in final edited form as:

*Methods Enzymol.* 2008 ; 446: 369–386. doi:10.1016/S0076-6879(08)01622-4.

## SYNTHESIS AND BIOPHYSICAL CHARACTERIZATION OF STABILIZED $\alpha$ -HELICES OF BCL-2 DOMAINS

Gregory H. Bird<sup>#</sup>, Federico Bernal<sup>#</sup>, Kenneth Pitter, and Loren D. Walensky

Department of Pediatric Oncology and the Program in Cancer Chemical Biology, Dana-Farber Cancer Institute, and the Division of Hematology/Oncology, Children's Hospital Boston, Harvard Medical School, Boston, Massachusetts

<sup>#</sup> These authors contributed equally to this work.

### Abstract

Rational design of compounds to mimic the functional domains of BCL-2 family proteins requires chemical reproduction of the biologic complexity afforded by the relatively large and folded surfaces of BCL-2 homology (BH) domain peptide  $\alpha$ -helices. Because the intermolecular handshakes of BCL-2 proteins are so critical to controlling cellular fate, we undertook the development of a toolbox of peptidic ligands that harness the natural potency and specificity of BH  $\alpha$ -helices to interrogate and potentially medicate the deregulated apoptotic pathways of human disease. To overcome the classic deficiencies of peptide reagents, including loss of bioactive structure in solution, rapid proteolytic degradation *in vivo*, and cellular impermeability, we developed a new class of compounds based on hydrocarbon stapling of BH3 death domain peptides. Here we describe the chemical synthesis of Stabilized Alpha-Helices of BCL-2 domains or SAHBs, and the analytical methods used to characterize their secondary structure, proteolytic stability, and cellular penetrance.

### 1. INTRODUCTION

The mission of chemical genetics is to identify compounds that directly and specifically alter protein function, so that physiologic activities can be investigated, and ultimately manipulated, on a conditional basis in real time. Identifying or generating such reagents to probe the broad range of apoptotic protein functions *in vitro* and specifically manipulate apoptotic pathways *in vivo* has been a significant and worthy challenge. Despite the obvious benefit of adopting “Nature’s solution” to target protein–protein interactions, peptides present significant biophysical and pharmacologic drawbacks, which include structural unfolding when taken out of context from the full-length protein and resultant loss of biologic activity, rapid proteolysis *in vivo*, and, except for a minority of peptides, the inability to penetrate intact cells. Because the peptide  $\alpha$ -helix participates in such a wide variety of intermolecular biologic recognition events, it is not surprising that a major focus of modern organic chemistry has been to devise synthetic strategies to recreate the architecture and stability of biologically active structures for both basic research and medicinal purposes.

An important strategic breakthrough in stabilizing  $\alpha$ -helices derived from installing a covalent bond between amino acids in an attempt to “lock” the peptide structure in place (Fig. 22.1) (Bracken et al., 1994; Jackson et al., 1991; Phelan et al., 1997). Initial successes

with covalent helix stabilization, however, involved both polar crosslinks, which impede cell permeability, and labile crosslinks, which are readily hydrolyzed by proteolytic enzymes (amides) or reduced (disulfides) (Fig. 22.1A,B). Grubbs and coworkers circumvented these drawbacks by forming a crosslink between *O*-allyl serine residues on adjacent turns of the  $\alpha$ -helix (Fig. 22.1C); the ring closing metathesis (RCM) chemistry uses a ruthenium catalyst to form a covalent bond between non-natural amino acid residues containing terminal double bonds or olefins (Blackwell and Grubbs, 1994). Ironically, although this chemical approach was successful in generating the covalent hydrocarbon crosslink, there was little to no enhancement of peptide  $\alpha$ -helicity. Subsequently, Verdine and colleagues developed an alternate approach that used  $\alpha,\alpha$ -disubstituted non-natural amino acids containing alkyl tethers (Fig. 22.1D) (Schafmeister et al., 2000). By experimenting with alternative placement of these non-natural amino acids along the peptide scaffold, in addition to varying stereochemistry and alkyl tether length, the chemical features required to dramatically stabilize a model helical peptide by use of an all-hydrocarbon chain crosslink were revealed. Here we describe the synthesis and biophysical characterization of stabilized  $\alpha$ -helices of BCL-2 domains (SAHBs), our first biologic application of the “peptide stapling” technology (Walensky et al., 2004).

## 2. SYNTHESIS OF NON-NATURAL AMINO ACIDS FOR PEPTIDE STAPLING

The asymmetric synthesis of the  $\alpha,\alpha$ -disubstituted amino acids required for peptide stapling is adapted from the method of Williams and colleagues (Fig. 22.2) (Williams and Im, 1991; Williams et al., 1988). The production of the Fmoc-protected crosslinking amino acid “S5” commences with the use of the Williams morpholinone (5*S*,6*R*)-4-*tert*-butoxycarbonyl-5,6-diphenyl-morpholin-2-one (**4**), which is commercially available (e.g., Sigma Aldrich) or can be generated from (1*R*,2*S*)-2-amino-1,2-diphenylethanol (**1**) as illustrated in Fig. 22.2 (**2**, **3**) and previously described in detail (Williams et al., 2003). The stereochemistry of the bulky phenyl groups dictates the chirality of the produced  $\alpha,\alpha$ -disubstituted amino acids. Installation of the helix-inducing  $\alpha$ -methyl group (Banerjee et al., 2002) is performed by deprotonating the  $\alpha$ -carbon of the morpholinone with sodium bis(trimethylsilyl)amide and alkylating with iodomethane at  $-78$  °C. The  $\alpha$ -methylated morpholinone, (5*S*,6*R*)-4-*tert*-butoxycarbonyl-5,6-diphenyl-3-methyl-morpholin-2-one (**5**), is obtained as a crystalline solid at a 3:2 ratio of diastereomers. The diastereomeric mixture of morpholinones is then treated with potassium bis(trimethylsilyl) amide in the presence of an alkenyl iodide (**7**) generated from a Finkelstein reaction of the bromide precursor (**6**). The second alkylation is performed at  $-42$  °C and cleanly produces the  $\alpha,\alpha$ -bisalkylated morpholinone, 3*S*,5*S*,6*R*-4-*tert*-butoxycarbonyl-5,6-diphenyl-3-methyl-3-(pent-4-enyl)-morpholin-2-one (**8**; *n*=1) in nearly quantitative yield with excellent diastereoselectivity (>98% *d.e.*) as determined by chiral HPLC.

After the synthesis of the bis-alkylated morpholinone, the chiral directing group is cleaved by reduction with lithium in liquid ammonia to yield the Boc-protected amino acid (*S*)-2-(*tert*-butoxycarbonylamino)-2-methyl-hept-6-enoic acid (**9**). Several methods exist for the cleavage of the C–N and C–O bonds in the morpholinone (Williams et al., 2003); however, dissolving metal reduction is the only method that is compatible with the compounds synthesized (Greenfield et al., 1954), as the alternative methods requiring reduction with H<sub>2</sub>

and palladium on carbon or oxidation with sodium periodate or lead (IV) tetraacetate would destroy the terminal olefin needed for the crosslinking reaction. To complete the synthesis, the Boc-protecting group on the  $\alpha$ -amine is converted to Fmoc to ensure compatibility with Fmoc solid-phase peptide synthesis. The Boc amino acid is dissolved in dichloromethane and exposed to excess trifluoroacetic acid to yield the free amine. Upon removal of the volatile components, the residue is dissolved in a 1:1 mixture of water and acetone and treated with sodium carbonate and *N*-(9-fluorenylmethoxycarbonyloxy)-succinimide (Fmoc-OSu) which yields, after column chromatography on silica gel, the desired Fmoc-protected amino acid (*S*)-2-(((9H-fluoren-9-yl)methoxy) carbonylamino)-2-methyl-hept-6-enoic acid (**10a**) in 75% yield. Whereas two S5 amino acids (**10a**) are used to generate ( $i, i + 4$ ) crosslinks, the R5 (**10b**) and (**10c**) (or S5 and R8) derivatives are used for ( $i, i + 7$ ) stapling. Once purified, the Fmoc-protected  $\alpha, \alpha$ -disubstituted amino acids are ready for use in solid-phase peptide synthesis.

### 3. DESIGN AND SYNTHESIS OF STABILIZED $\alpha$ -HELICES OF BCL-2 DOMAINS (SAHBs)

The BH3 domains of many BCL-2 family members have been structurally defined as amphipathic  $\alpha$ -helices (Chou et al., 1999; Day et al., 2005; Denisov et al., 2003; Hinds et al., 2003; McDonnell et al., 1999; Muchmore et al., 1996; Petros et al., 2000; 2001; Sattler et al., 1997; Suzuki et al., 2000). Whereas the hydrophobic face of the  $\alpha$ -helix contacts a hydrophobic pocket of its interacting partner, charged residues on the hydrophilic face participate in electrostatic pairings with the target protein in addition to being exposed to the aqueous environment (Sattler et al., 1997). When designing the insertion points for hydrocarbon staples, assessment of available structural data is ideal so that native amino acids essential to protein interaction can be preserved. For example, the alanine scan performed by Sattler *et al.* for the interaction between BAK BH3 and BCL-X<sub>L</sub> C determined the important hydrophobic and charged amino acids for BH3 engagement (Sattler et al., 1997). Thus, in this example, the S5 amino acid is specifically implanted in ( $i, i + 4$ ) pairings that do not disrupt key interacting residues of the hydrophobic contact surface (Fig. 22.3).

The construction of a stapled BH3 peptide can be performed either manually or by use of an automated peptide synthesizer (Fig. 22.4). In either case, the solid-phase synthesis resin of choice (e.g., Rink amide MB HA resin with loading levels of 0.4 to 0.6 mmol/g resin) is swollen with 1-methyl-2-pyrrolidinone (NMP) for 15 min. After draining, the Fmoc group is deprotected by exposure to a 20% (v/v) solution of piperidine in NMP for 30 min. After extensive washing with NMP, the resin beads are exposed first to a 0.5 M solution of amino acid in NMP, followed by a 0.5 M solution of 2-(6-chloro-1*H*-benzotriazole-1-yl)-1,1,3,3-tetramethylaminium hexafluorophosphate (HCTU) coupling agent (Albericio, 2004). The resin is then treated with *N,N*-diisopropyl ethylamine (DIEA), and the reaction is carried out for 30 to 60 min with either shaking or bubbling under nitrogen. Typically, 4 equivalents of Fmoc-amino acid, 3.9 equivalents of coupling agent, and 8 equivalents of DIEA are used, and double couplings are performed. After completion of the peptide synthesis, the amino terminus can either be acetylated by reaction with acetic anhydride and DIEA or subjected to alternative derivatization (e.g., FITC- $\beta$ -Ala, biotin- $\beta$ -Ala). For amino terminal modifications that contain such sulfur atoms, the  $\beta$ -Ala can be installed at this stage but

FITC or biotin capping is deferred until after metathesis to avoid sulfur-based poisoning of the ruthenium catalyst.

The olefin metathesis step is carried out by first swelling the resin with 1,2-dichloroethane followed by exposure to a 10 mM solution of bis(tricyclohexylphosphine)-benzylidene ruthenium (IV) dichloride (Grubbs' first generation catalyst) in 1,2-dichloroethane (0.20 mol % on the basis of resin substitution) for 2 h. The stapling reaction is carried out twice with constant bubbling under nitrogen. The resin-bound peptide is then washed with 1,2-dichloroethane three times and dried under a stream of nitrogen. Sulfur-containing moieties can be *N*-terminally appended at this stage after Fmoc deprotection in piperidine. The completed peptide is cleaved from the resin and deprotected by exposure to trifluoroacetic acid (TFA)-based cleavage cocktails such as reagent K (82.5% TFA, 5% thioanisole, 5% phenol, 5% water, 2.5% 1, 2-ethanedithiol) or TFA/triisopropyl silane (TIS)/water (95%, 2.5%, 2.5%), and precipitated with methyl-*tert*-butyl ether at 4 °C followed by lyophilization.

Lyophilized SAHB peptides are purified by reverse-phase HPLC by use of a C<sub>18</sub> column. The compounds are characterized by LC/MS, with mass spectra obtained either by electrospray in positive ion mode or by MALDI-TOF. Quantitation is achieved by amino acid analysis on a Beckman 6300 high-performance amino acid analyzer. Working stock solutions are generated by dissolving the lyophilized material in DMSO at 1 to 10 mM. Lyophilized powder and DMSO stock solutions are stored at -20 °C.

#### 4. STRUCTURAL ASSESSMENT OF SAHBs BY CIRCULAR DICHROISM (CD)

To evaluate secondary structure improvements of hydrocarbon-stapled BH3 peptides, CD spectra are recorded and analyzed. Generally, short peptides do not exhibit significant  $\alpha$ -helical structure in solution because the entropic cost of maintaining a conformationally restricted structure is not overcome by the enthalpic gain from hydrogen bonding of the peptide backbone. Indeed, we find that unmodified BH3 peptides, ranging in length from 16 to 25 amino acids, display  $\alpha$ -helical propensities of less than 25% (Letai et al., 2002), whereas installation of a chemical staple typically enhances  $\alpha$ -helicity by 3- to 5-fold (Fig. 22.5) (Walensky et al., 2004; 2006).

CD spectra are recorded on an Aviv Biomedical spectrometer (Model 410) equipped with a Peltier temperature controller and a thermoelectric sample changer with 5-position rotor. A total of five scans from 190 to 260 nm in 0.5-nm increments with 0.5 sec averaging time are collectively averaged to obtain each spectrum using a 1-mm path length cell. For temperature scans, three scans are averaged at temperature increments of 5 °C from 1 °C to 91 °C. The target peptide concentration is 25 to 50  $\mu$ M, and exact concentrations are confirmed by quantitative amino acid analysis of two CD sample dilutions. It is important to carefully assess compound solubility by first dissolving the peptide in buffer followed by high-speed tabletop centrifugation to ensure that there is no pellet. SAHBs are generally reconstituted in 5 mM potassium phosphate (pH 7.5) or Milli-Q deionized water, but alternate aqueous buffers spanning a wider pH range or organic co-solvents may be required to optimize solubility.

The CD spectra are initially plotted as wavelength vs millidegree, the default output of the instrument. Once the precise peptide concentration is confirmed, the mean residue ellipticity  $[\theta]$ , in units of degree  $\text{cm}^2 \text{dmol}^{-1} \text{residue}^{-1}$ , is derived from Eq. (22.1):

$$[\theta] = \text{millidegree/molar concentration/number of amino acid residues} \quad (22.1)$$

Once converted to mean residue ellipticity, percent  $\alpha$ -helicity can be calculated with Eqs. (22.2) and (22.3)(Forood et al., 1993):

$$\% \text{Helicity} = 100 \times [\theta]_{222} / [\theta]_{222}^{\text{max}} \text{ where} \quad (22.2)$$

$$[\theta]_{222}^{\text{max}} = -40,000 \times [1 - (2.5/\text{number of amino acid residues})] \quad (22.3)$$

Alternately, most CD instruments are bundled with curve-fitting software programs, such as CDDN (Bohm et al., 1992), that deduce the relative fractions of secondary structure including  $\alpha$ -helix, parallel and antiparallel  $\beta$ -sheet,  $\beta$ -turn, and random coil.

## 5. PROTEASE RESISTANCE TESTING OF SAHBs

Protein degradation *in vivo* is a natural metabolic process that activates and deactivates biologically active peptides in a regulated, homeostatic fashion. Peptide proteolysis, however, remains a major hurdle for the conversion of synthetic peptides to pharmaceuticals. One of the benefits of enforcing peptide  $\alpha$ -helicity is the shielding of the vulnerable amide bond from *in vivo* proteolysis. Because proteases require that peptides adopt an extended conformation to hydrolyze amide bonds, the structural constraint afforded by the hydrocarbon staple renders the crosslinked peptides protease-resistant. To measure and optimize SAHB stability, we use several proteolytic stability assays.

### 5.1. *In vitro* trypsin/chymotrypsin degradation assay

To assess protease resistance *in vitro*, proteolytic enzymes are selected based on the sequence composition of the peptide substrate, such that effective fragmentation can be achieved. Trypsin, which recognizes Arg and Lys, and chymotrypsin, which predominantly cleaves after Phe, Tyr, Trp, Leu, Met, are commonly used. Several experimental and analytical approaches can be undertaken. For example, relative stability of a FITC-labeled unmodified and stapled peptide can be compared by exposing the compounds (e.g., 5  $\mu\text{g}$ ) to trypsin agarose (Pierce) (substrate/enzyme  $\approx 125$ ) overtime (e.g., 0, 10, 20, 90, and 180 min) (Fig. 22.6A). Reactions are quenched by tabletop centrifugation at high speed, and remaining full-length substrate in the isolated supernatant is analyzed by HPLC-based quantitation with fluorescence detection at excitation/emission settings of 495/530 nm.

Alternately, mass spectrometry-based quantitation can be used to increase sensitivity and avoid the use of *N*-terminally derivatized FITC SAHBs. MS/MS-based detection and

quantitation is typically used in pharmacokinetic studies of stability and metabolism to eliminate signal suppression from complex mixtures; however, a standard single-quadripole mass spectrometer detector found in most academic institutions is also capable of quantifying intact peptide in an *in vitro* assay consisting of enzyme and peptide dissolved in a phosphate-buffered calcium chloride solution. For example, we use an Agilent model 1200 LC/MS with the following settings: 20  $\mu$ l injection, 0.6 ml flow rate, a gradient of water (0.1% formic acid) to 20 to 80% acetonitrile (0.075% formic acid) over 10 min, with 4 min at completion to revert to starting gradient conditions and 0.5 min post-time, allowing for an overall 15-min run time. The diode-array detector (DAD) signal is set to 280 nm with an 8 nm bandwidth. Mass spectrometry detector (MSD) settings are in scan mode with one channel gated on  $(M + 2H)/2, \pm 1$  mass unit and the other on  $(M + 3H)/3, \pm 1$  mass unit. Integration of each MSD signal typically yields counts for area under the curve of  $\sim 10^8$ . Because each run takes 15 min, four duplicate samples can be staggered such that four data points are acquired per hour, with the proteolytic enzyme promptly added to the sample once the zero-hour time point is autoinjected. Plotting of MSD area vs time generates an exponential decay curve with error bars typically 5% or less. An internal control of acetylated tryptophan carboxamide at a concentration of 100  $\mu$ M can be used with absorbance at 278 nm to normalize each MSD data point.

## 5.2. Serum stability assays

To extend the proteolytic analysis to *in vitro* and *in vivo* serum stability, peptides (e.g., 2.5 to 5  $\mu$ g) are incubated with fresh mouse serum (e.g., 25  $\mu$ l) at 37 °C or injected (e.g., 10 mg/kg) by tail vein into mice, respectively. *Ex vivo* serum samples or serum isolated from serial tail bleeds (e.g., 25  $\mu$ L) are collected at various time intervals (e.g., 0, 1, 2, 4, 8, and 24 h), flash frozen, lyophilized, and then extracted with acidified organic solvent solution (e.g., 50:50 acetonitrile/water containing 0.1% trifluoroacetic acid). Levels of intact peptide are detected and quantified as described in section 5.1 (Fig. 22.6B,C).

## 6. CELL PERMEABILITY SCREENING OF SAHBs

Despite the exquisite biologic specificity of native peptides for their protein targets, a major limitation of peptides as therapeutics is their general inability to cross lipid membranes to access the intracellular environment. The charge of amino acid side chains and the polarity of the peptide backbone account for the impenetrability. However, a discrete subclass of cationic peptides (e.g., HIV-TAT, penetratin sequence from the *Antennapedia* homeodomain, poly-Arg), termed cell penetrating peptides or CPPs, have been shown to enter cells (Derossi et al., 1994; Fawell et al., 1994; Schwarze et al., 1999) by an energy-dependent fluid-phase macropinocytosis mechanism (Wadia et al., 2004). Hydrocarbon-stapled BH3 peptides were likewise found to be cell permeable through a pinocytotic pathway, although in contrast to cationic CPPs, initial contact with the plasma membrane does not seem to be mediated by interactions with glycosaminoglycans (Console et al., 2003; Walensky et al., 2004). The cell penetrability of SAHBs is believed to derive from the reinforced  $\alpha$ -helical structure of the peptides, as peptide helices are common membrane-interacting protein motifs; the hydrophobicity of the hydrocarbon staple itself may additionally contribute to membrane tropism. To evaluate the cellular uptake of SAHB compounds, we use two assays in

combination: FACS analysis and confocal microscopy of FITC-SAHB treated cells. In general, neutral to cationic SAHBs consistently display efficient cellular uptake (Console et al., 2003; Walensky et al., 2004; 2006), whereas anionic species may require sequence modification (e.g., point mutagenesis, sequence shift) to dispense with negative charge (Bernal et al., 2007).

### 6.1. FACS analysis of FITC-SAHB-treated cells

SAHBs are diluted in stepwise fashion from 100% DMSO stock solutions (1 to 10 mM) into water, with the experimental concentration (e.g., 1 to 10  $\mu$ M) achieved by final dilution into serum-free tissue culture media. It is important to monitor the treatment solutions for any sign of compound precipitation, which can be avoided by modifying the media solution (e.g., increasing final DMSO concentration to 1 or 2%). Nonadherent cells are washed in serum-free media and diluted to a concentration of  $1 \times 10^6$  cells/ml, and typically 50  $\mu$ l (50,000 cells) are combined with 50  $\mu$ l of FITC-SAHB solution (e.g., 5, 10, and/or 20  $\mu$ M) concentration and incubated at 37 °C. The corresponding unmodified FITC-peptide is used as a negative control. After 4 h or serial time points, the cells are pelleted at 1400 rpm on a tabletop swinging bucket centrifuge for 4 min, and the supernatant is gently aspirated. The cells are incubated in 50  $\mu$ l of tissue-culture grade trypsin solution (e.g., 0.25%, Gibco) to cleave surface proteins and thereby help eliminate any nonspecifically bound peptide from the cell surface. After 5 min, the trypsin is quenched with 300  $\mu$ l of media containing 10% FBS. The cells are then pelleted again, washed in PBS, pelleted, and resuspended in 200  $\mu$ l of FACS buffer. The procedure is identical for adherent cells, except that 50,000 cells are replated in serum-containing media and then, at the outset of the experiment, washed twice in serum-free media; the cells are detached from the culture plates during the trypsinization step described previously. Cellular fluorescence is analyzed by use of a FACSCalibur flow cytometer (Becton Dickinson) and FlowJo software (Tree Star) (Fig. 22.7A). FITC intensity is detected on a log scale, and 10,000 cells are counted per treatment replicate. To exclude membrane disruption as the mechanism for cellular entry and fluorescence, cell permeabilization can be evaluated by adding 0.5  $\mu$ g/ml propidium iodide (BD Biosciences) to the analyzed samples. To evaluate an endocytic mechanism of import, the identical experiment can be performed with: (a) 30 min preincubation of cells at 4 °C followed by 4 h incubation with FITC-compounds at 4 °C to assess temperature-dependence of fluorescent labeling; (b) 60 min pretreatment of cells at 37 °C with 10 mM sodium azide and 50 mM 2-deoxy-D-glucose to deplete cellular ATP and thereby assess energy-dependence of fluorescent labeling (Potocky et al., 2003; Richard et al., 2003).

### 6.2. Confocal microscopy of FITC-SAHB-treated cells

Whereas the FACS-based cell permeability assay is amenable to rapid screening of compounds, it is not meant to stand alone as proofpositive of cellular uptake. Confirmatory testing with confocal microscopy of FITC-SAHB-treated cells is used to demonstrate intracellular fluorescence and subcellular localization. Cells are incubated with FITC-labeled compounds in serum-free media for up to 4 h as described previously or with serum replacement (as 2 $\times$  serum-containing media) followed by additional incubation intervals (e.g., 20 h) at 37 °C. In preparation for fixation, nonadherent cells are washed twice with PBS and then cytopun at 600 rpm for 5 min onto Superfrost plus glass slides (Fisher);

media is aspirated from the wells of adherent cells and then washed twice with PBS *in situ*. Slides are exposed to freshly prepared 4% paraformaldehyde/PBS, washed with PBS, incubated with a nuclear counterstain (e.g., 100 nM TO-PRO-3 iodide [Molecular Probes]), treated with Vectashield mounting medium (Vector), and then imaged by confocal microscopy (BioRad 1024) (Fig. 22.7B). For double-labeling experiments to identify subcellular compartments, fixed cells can be incubated with a primary antibody (e.g., Tom20 for outer mitochondrial membrane labeling [Schleiff et al., 1997]) and rhodamine-conjugated secondary antibody before nuclear counterstaining. Because cationic CPPs have been shown to relocalize during cellular fixation (Drin et al., 2003; Richard et al., 2003), live confocal microscopy can be used to further confirm the intracellular localization of FITC-SAHB compounds. Cells doubly labeled with FITC-SAHB and live cell organellar markers (e.g., 100 nM MitoTracker [Molecular Probes]) are washed and resuspended in PBS, followed by wet mount preparation and prompt confocal microscopy analysis.

## 7. SUMMARY

Novel chemical approaches that optimize the pharmacology and bioactivity of peptides are rejuvenating the field of peptide therapeutics. Moreover, chemical reconstitution of native peptide structures has yielded new biologic tools to interrogate signal transduction pathways *in vitro* and *in vivo*. In this case, the application of hydrocarbon stapling to BH domain peptides has enabled the synthesis of compounds with structural fidelity, proteolytic stability, and cell permeability, thereby facilitating the biochemical analysis and pharmacologic manipulation of BCL-2 family protein interactions. The application of SAHB compounds to apoptosis research is the subject of a separate chapter.

## ACKNOWLEDGMENTS

We thank E. Smith for figure design and editorial assistance, Gregory L. Verdine and the late Stanley J. Korsmeyer for their invaluable mentorship, members of the Walensky laboratory, past and present, for their scientific contributions, and C. E. Schafmeister, J. Po, and I. Escher, former members of the Verdine laboratory, for their seminal work on the allhydrocarbon crosslinking system. L. D. W. is supported by NIH grants K08HL074049, 5R01CA50239, and 5P01CA92625, a Burroughs Wellcome Fund Career Award in the Biomedical Sciences, a Partnership for Cures Charles E. Culpeper Scholarship in Medical Science, a grant from the William Lawrence Children's Foundation, and the Dana-Farber Cancer Institute High-Tech fund. G.H.B. is the recipient of a Harvard University Center for AIDS Research Scholar Award and F.B. is funded by a grant from the Dana. Farber Cancer Institute Pediatric Low-Grade Astrocytoma Program.

## REFERENCES

- Albericio F (2004). Developments in peptide and amide synthesis. *Curr. Opin. Chem. Bio* 8, 211–221. [PubMed: 15183318]
- Banerjee R, Basu G, Chene P, and Roy S (2002). Aib-based peptide backbone as scaffolds for helical peptide mimics. *J. Pept. Res* 60, 88–94. [PubMed: 12102721]
- Bernal F, Tyler AF, Korsmeyer SJ, Walensky LD, and Verdine GL (2007). Reactivation of the p53 tumor suppressor pathway by a stapled p53 peptide. *J. Am. Chem. Soc* 129, 2456–2457. [PubMed: 17284038]
- Blackwell HE, and Grubbs RH (1994). Highly Efficient Synthesis of Covalently Cross-Linked Peptide Helices by Ring-Closing Metathesis. *Angew Chem. Int. Ed* 37, 3281–3284.
- Bohm G, Muhr R, and Jaenicke R (1992). Quantitative-Analysis of Protein Far Uv Circular-Dichroism Spectra by Neural Networks. *Protein Eng.* 5, 191–195. [PubMed: 1409538]



- Bracken C, Gulyas J, Taylor JW, and Baum J (1994). Synthesis and nuclear magnetic resonance structure determination of an alpha-helical, bicyclic, lactam-bridged hexapeptide. *J. Am. Chem. Soc* 116, 6431–6432.
- Chou JJ, Li H, Salvesen GS, Yuan J, and Wagner G (1999). Solution structure of BID, an intracellular amplifier of apoptotic signaling. *Cell* 96, 615–624. [PubMed: 10089877]
- Console S, Marty C, Garcia-Echeverria C, Schwendener R, and Ballmer-Hofer K (2003). Antennapedia and HIV transactivator of transcription (TAT) “protein transduction domains” promote endocytosis of high molecular weight cargo upon binding to cell surface glycosaminoglycans. *J. Biol. Chem* 278, 35109–35114. [PubMed: 12837762] ,
- Day CL, Chen L, Richardson SJ, Harrison PJ, Huang DC, and Hinds MG (2005). Solution structure of pro-survival Mcl-1 and characterization of its binding by proapoptotic BH3-only ligands. *J. Biol. Chem* 280, 4738–4744. [PubMed: 15550399]
- Denisov AY, Madiraju MS, Chen G, Khadir A, Beauparlant P, Attardo G, Shore GC, and Gehring K (2003). Solution Structure of Human BCL-w: Modulation of ligand binding by the C-terminal helix. *J. Biol. Chem* 278, 21124–21128. [PubMed: 12651847]
- Derossi D, Joliot AH, Chassaing G, and Prochiantz A (1994). The third helix of the Antennapedia homeodomain translocates through biological membranes. *J. Biol. Chem* 269, 10444–10450. [PubMed: 8144628]
- Drin G, Cottin S, Blanc E, Rees AR, and Tamsamani J (2003). Studies on the internalization mechanism of cationic cell-penetrating peptides. *J. Biol. Chem* 278, 31192–31201. [PubMed: 12783857]
- Fawell S, Seery J, Daikh Y, Moore C, Chen LL, Pepinsky B, and Barsoum J (1994). Tat-mediated delivery of heterologous proteins into cells. *Proc. Natl. Acad. Sci. USA* 91, 664–668. [PubMed: 8290579]
- Forood B, Feliciano EJ, and Nambiar KP (1993). Stabilization of Alpha-Helical Structures in Short Peptides Via End Capping. *Proc. Nat Acad. Sci. USA* 90, 838–842. [PubMed: 8430094]
- Greenfield H, Friedel RA, and Orchin M (1954). The reduction of simple olefins with sodium and methanol in liquid ammonia. 76, 1258–1259.
- Hinds MG, Lackmann M, Skea GL, Harrison PJ, Huang DC, and Day CL (2003). The structure of Bcl-w reveals a role for the C-terminal residues in modulating biological activity. *EMBO J.* 22, 1497–1507. [PubMed: 12660157] ,
- Jackson DY, King DS, Chmielewski J, Singh S, and Schultz PG (1991). General approach to the synthesis of short  $\alpha$ -helical peptides. *J. Am. Chem. Soc* 113, 9391–9392.
- Letai A, Bassik MC, Walensky LD, Sorcinelli MD, Weiler S, and Korsmeyer SJ (2002). Distinct BH3 domains either sensitize or activate mitochondrial apoptosis, serving as prototype cancer therapeutics. *Cancer Cell* 2, 183–192. [PubMed: 12242151] ,
- McDonnell JM, Fushman D, Milliman CL, Korsmeyer SJ, and Cowburn D (1999). Solution structure of the proapoptotic molecule BID: A structural basis for apoptotic agonists and antagonists. *Cell* 96, 625–634. [PubMed: 10089878]
- Muchmore SW, et al. (1996). X-ray and NMR structure of human Bcl-xL, an inhibitor of programmed cell death. *Nature* 381, 335–341. [PubMed: 8692274]
- Petros AM, Medek A, Nettesheim DG, Kim DH, Yoon HS, Swift K, Matayoshi ED, Oltersdorf T, and Fesik SW (2001). Solution structure of the antiapoptotic protein bcl-2. *Proc. Natl. Acad. Sci. USA* 98, 3012–3017. [PubMed: 11248023]
- Petros AM, Nettesheim DG, Wang Y, Olejniczak ET, Meadows RP, Mack J, Swift K, Matayoshi ED, Zhang H, Thompson CB, and Fesik SW (2000). Rationale for Bcl-xL/Bad peptide complex formation from structure, mutagenesis, and biophysical studies. *Protein Sci.* 9, 2528–2534. [PubMed: 11206074] ,
- Phelan JC, Skelton NJ, Braisted AC, and McDowell RS (1997). A general method for constraining short peptides to an  $\alpha$ -helical conformation. *J. Am. Chem. Soc* 119, 455–460.,
- Potocky TB, Menon AK, and Gellman SH (2003). Cytoplasmic and nuclear delivery of a TAT-derived peptide and a beta-peptide after endocytic uptake into HeLa cells. *J. Biol. Chem* 278, 50188–50194. [PubMed: 14517218]

- Richard JP, Melikov K, Vives E, Ramos C, Verbeure B, Gait MJ, Chernomordik LV, and Lebleu B (2003). Cell-penetrating peptides. A reevaluation of the mechanism of cellular uptake. *J. Biol. Chem* 278, 585–590. [PubMed: 12411431] ,
- Sattler M, et al. (1997). Structure of Bcl-xL-Bak peptide complex: Recognition between regulators of apoptosis. *Science* 275, 983–986. [PubMed: 9020082]
- Schafmeister C, Po J, and Verdine G (2000). An all-hydrocarbon cross-linking system for enhancing the helicity and metabolic stability of peptides. *J. Am. Chem. Soc* 122, 5891–5892.
- Schleiff E, Shore GC, and Goping IS (1997). Interactions of the human mitochondrial protein import receptor, hTom20, with precursor proteins *in vitro* reveal pleiotropic specificities and different receptor domain requirements. *J. Biol. Chem* 272, 17784–17789. [PubMed: 9211931]
- Schwarze SR, Ho A, Vocero-Akbani A, and Dowdy SF (1999). *In vivo* protein transduction: Delivery of a biologically active protein into the mouse. *Science* 285, 1569–1572. [PubMed: 10477521]
- Suzuki M, Youle RJ, and Tjandra N (2000). Structure of Bax: Coregulation of dimer formation and intracellular localization. *Cell* 103, 645–654. [PubMed: 11106734]
- Wadia JS, Stan RV, and Dowdy SF (2004). Transducible TAT-HA fusogenic peptide enhances escape of TAT-fusion proteins after lipid raft macropinocytosis. *Nat. Med* 10, 310–315. [PubMed: 14770178]
- Walensky LD, Kung AL, Escher I, Malia TJ, Barbuto S, Wright RD, Wagner G, Verdine GL, and Korsmeyer SJ (2004). Activation of apoptosis *in vivo* by a hydrocarbon-stapled BH3 helix. *Science* 305, 1466–1470. [PubMed: 15353804]
- Walensky LD, Pitter K, Morash J, Oh KJ, Barbuto S, Fisher J, Smith E, Verdine GL, and Korsmeyer SJ (2006). A stapled BID BH3 helix directly binds and activates BAX. *Mol. Cell* 24, 199–210. [PubMed: 17052454]
- Williams RM, and Im MN (1991). Asymmetric synthesis of monosubstituted and alpha, alpha-disubstituted amino acids via diastereoselective glycine enolate alkylations. *J. Am. Chem. Soc* 113, 9276–9286.,
- Williams RM, Sinclair PJ, Zhai D, and Chen D (1988). Practical asymmetric syntheses of alpha-amino acids through carbon-carbon bond constructions on electrophilic glycine templates. *J. Am. Chem. Soc* 110, 1547–1557.,
- Williams RM, Sinclair PJ, DeMong DE, Chen D, and Zhai D (2003). Asymmetric Synthesis of N-tert-butoxycarbonyl Alpha-Amino Acids: Synthesis of (5S, 6R)-4-tert-butoxycarbonyl-5,6-diphenylmorpholin-2-one. *Organic Syntheses* 80, 18–30.

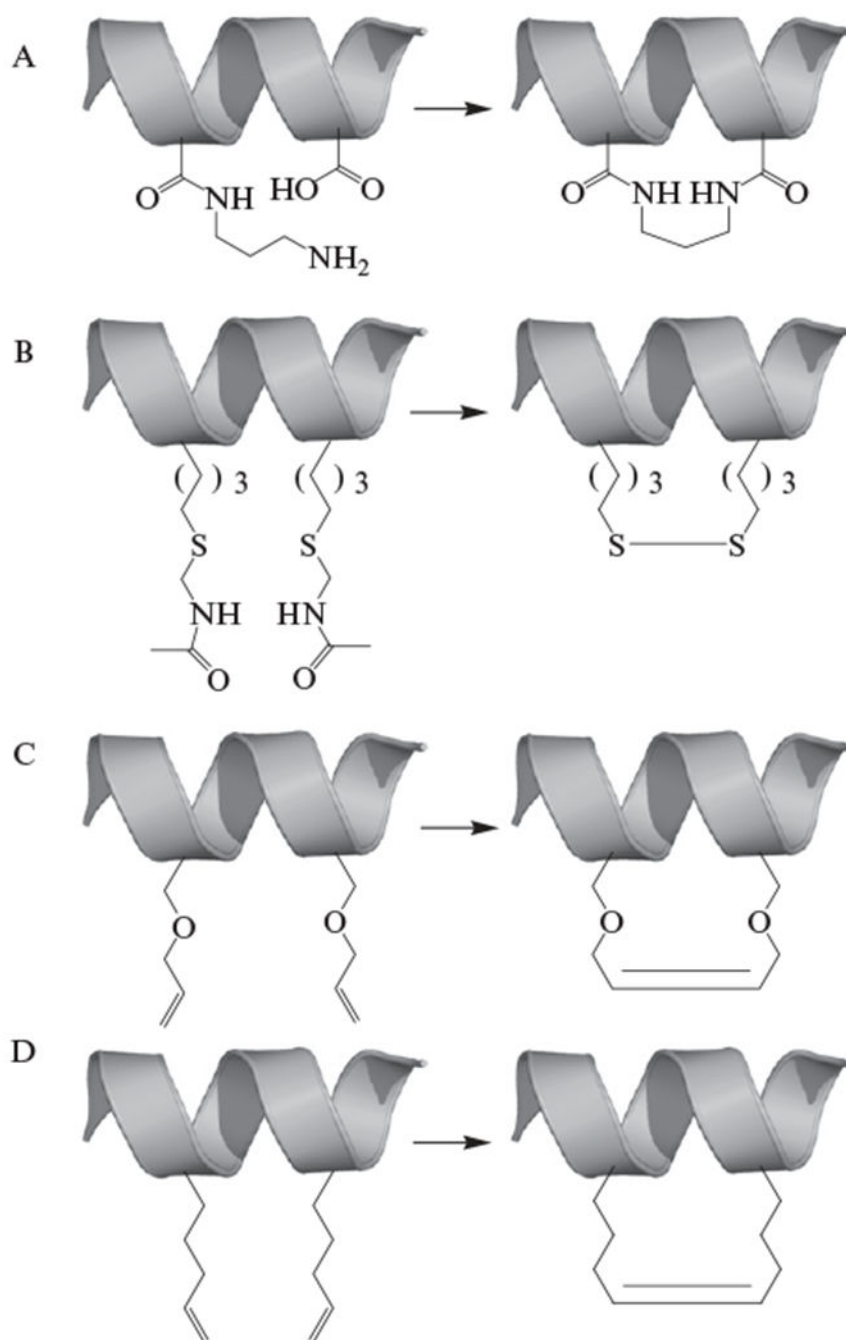


**Figure 22.1.** Approaches to covalent  $\alpha$ -helical stabilization have included the use of (A) lactam bridges, (B) disulfide bridges, (C) ruthenium-catalyzed ring closing metathesis (RCM) of O-allyl serine residues, and (D) RCM of  $\alpha, \alpha$ -disubstituted non-natural amino acids bearing alkyl tethers.

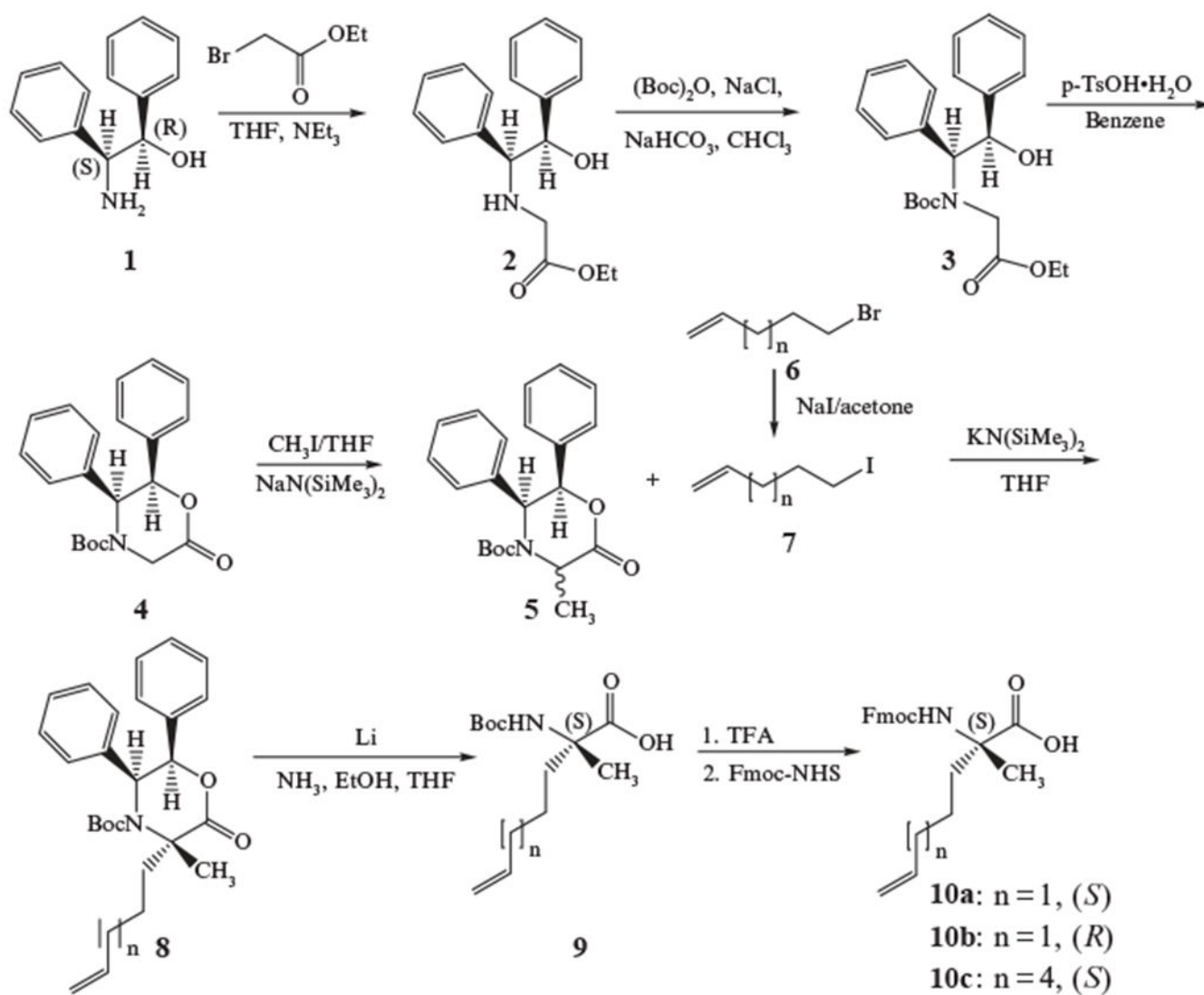


**Figure 22.2.** Synthetic scheme for generating the chiral  $\alpha,\alpha$ -disubstituted non-natural amino acids used to staple bioactive peptides.

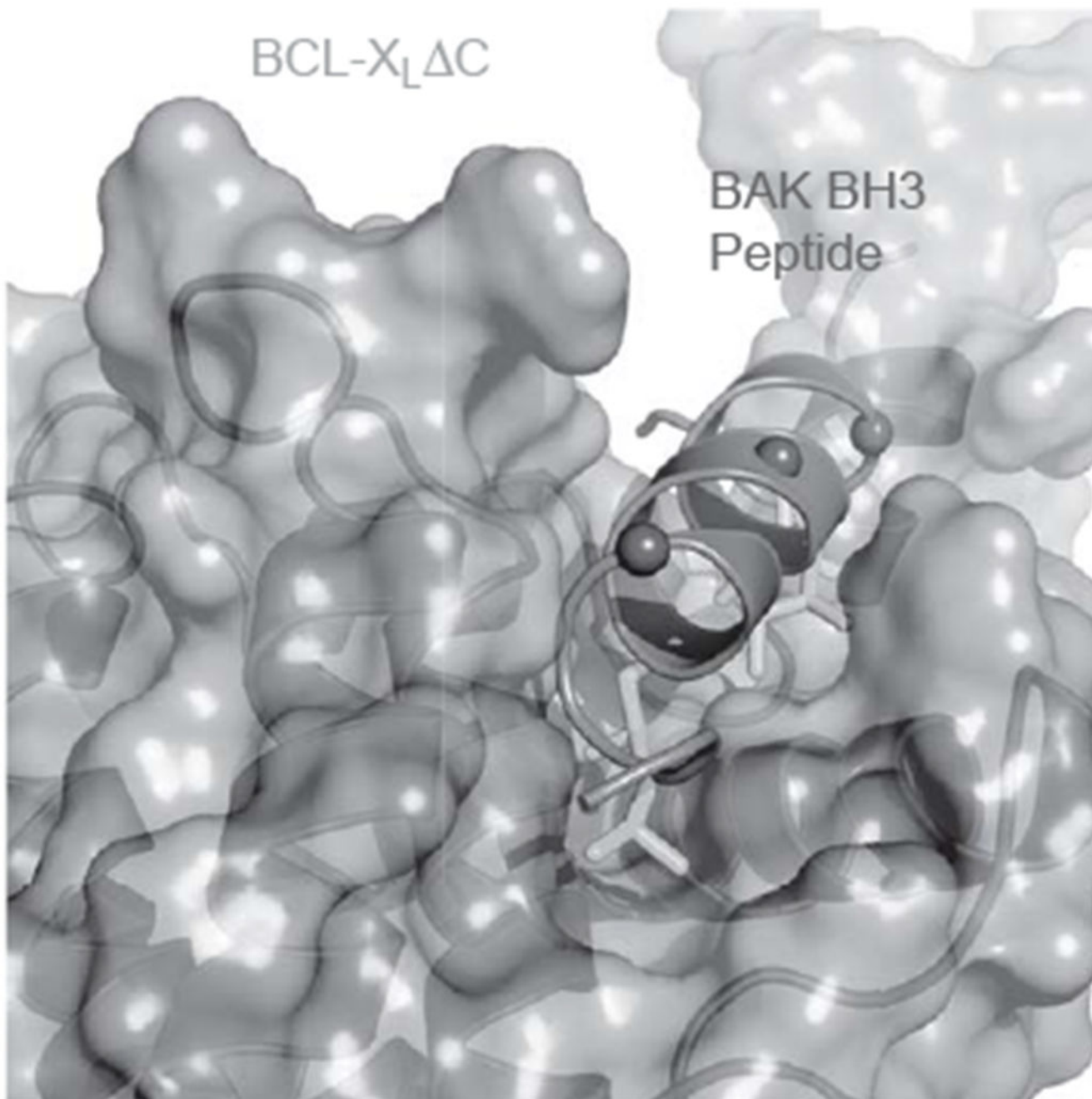


**Figure 22.3.** Design considerations for installing hydrocarbon staples derive from structural data (e.g., BAK BH3/BCL-XL C; PDB 1BXL [Sattler et al., 1997]) that highlight key interacting surfaces to be avoided. Several ( $i, i + 4$ ) residues indicated as red balls on the noninteracting surface of the BAK BH3 helix are amenable to replacement with the S5 non-natural amino acid.

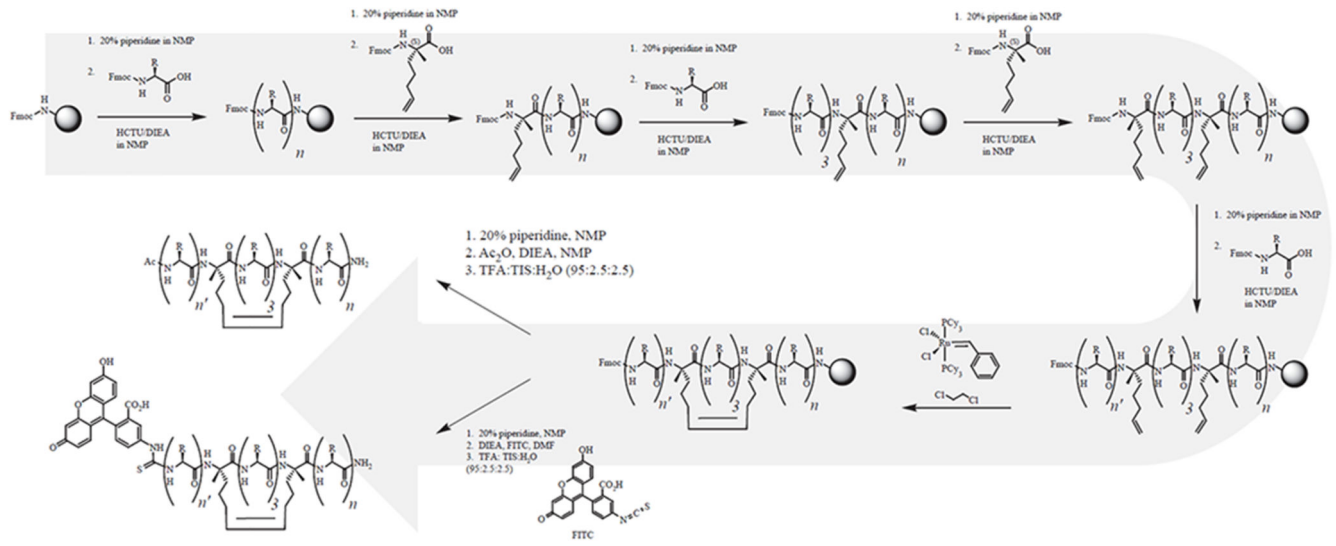


**Figure 22.4.** Synthetic scheme for the generation of SAHBs by Fmoc-based solid-phase peptide synthesis and ruthenium-catalyzed olefin metathesis.

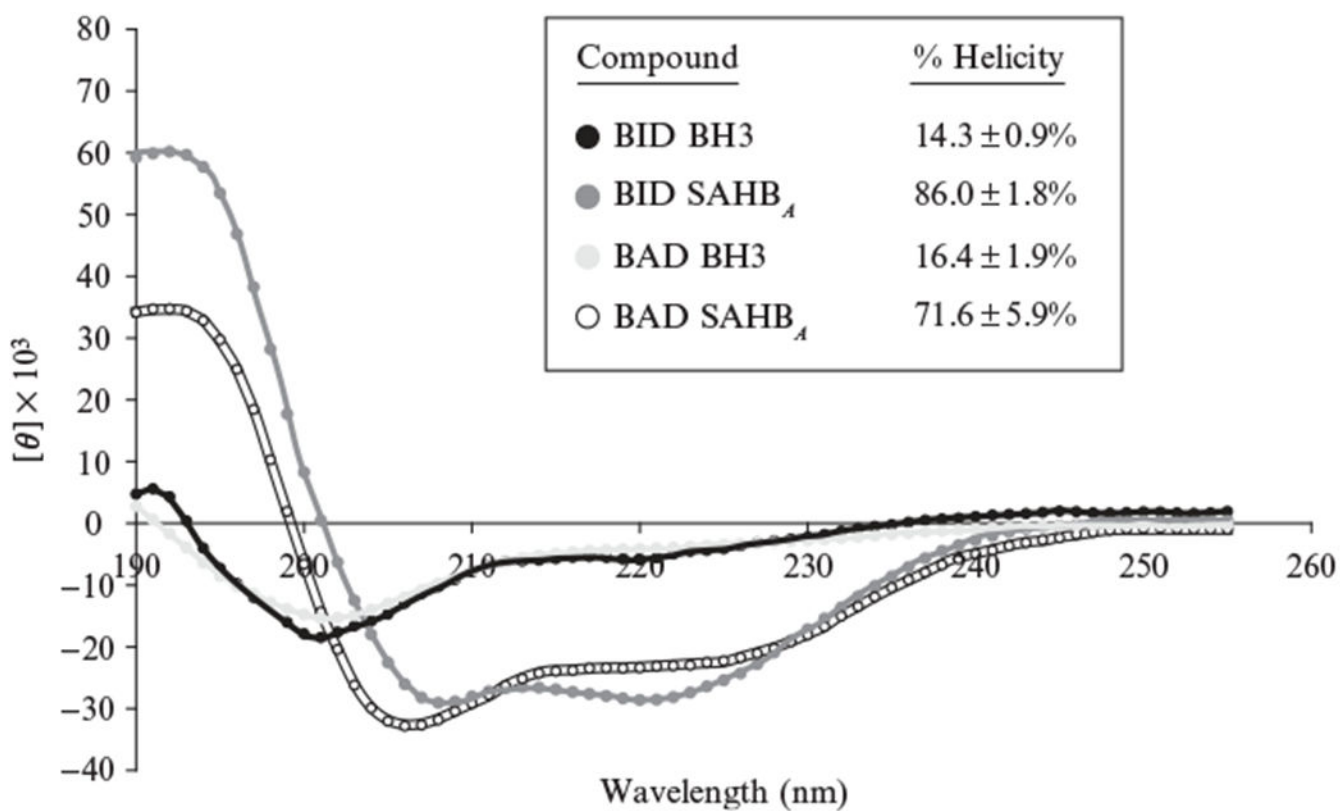


**Figure 22.5.** Circular dichroism spectra demonstrate the increased  $\alpha$ -helicity of SAHBs compared to the corresponding unmodified BH3 peptides (Walensky et al., 2006).

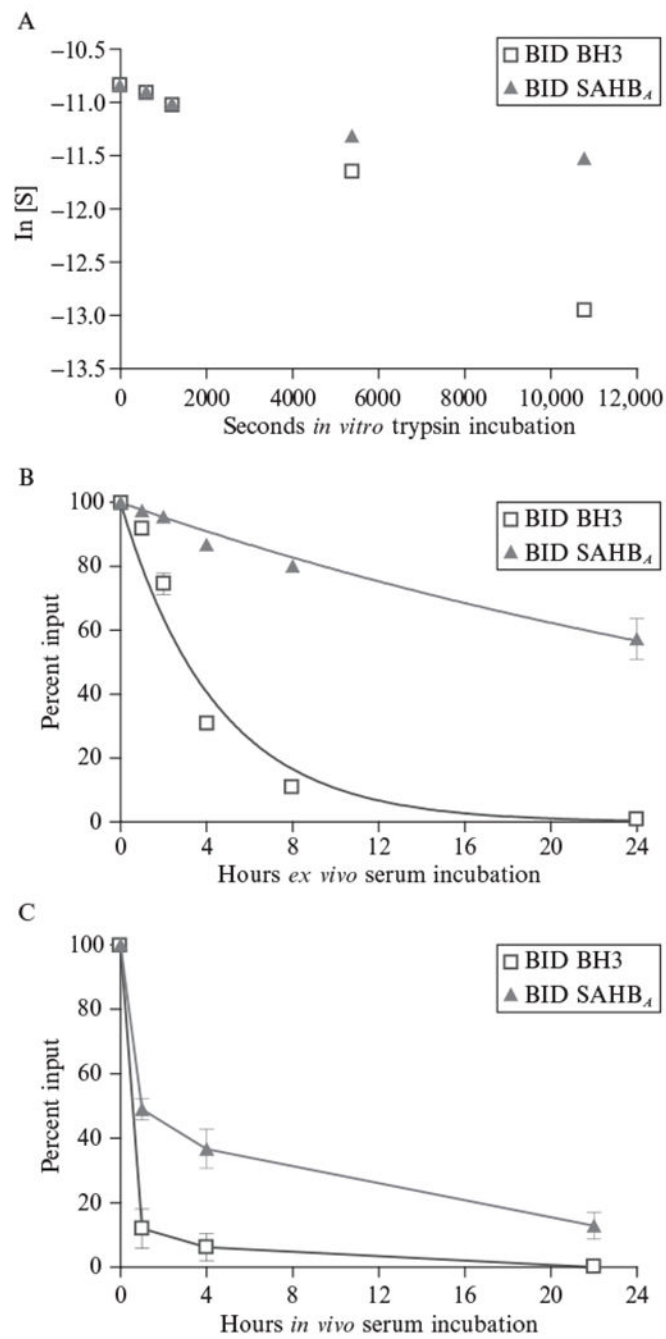


**Figure 22.6.** SAHBs exhibit marked protease resistance compared with unmodified BH3 peptides as assessed by (A) *in vitro* trypsin degradation assay, (B) *ex vivo*, and (C) *in vivo* serum stability assays (Walensky et al., 2004).



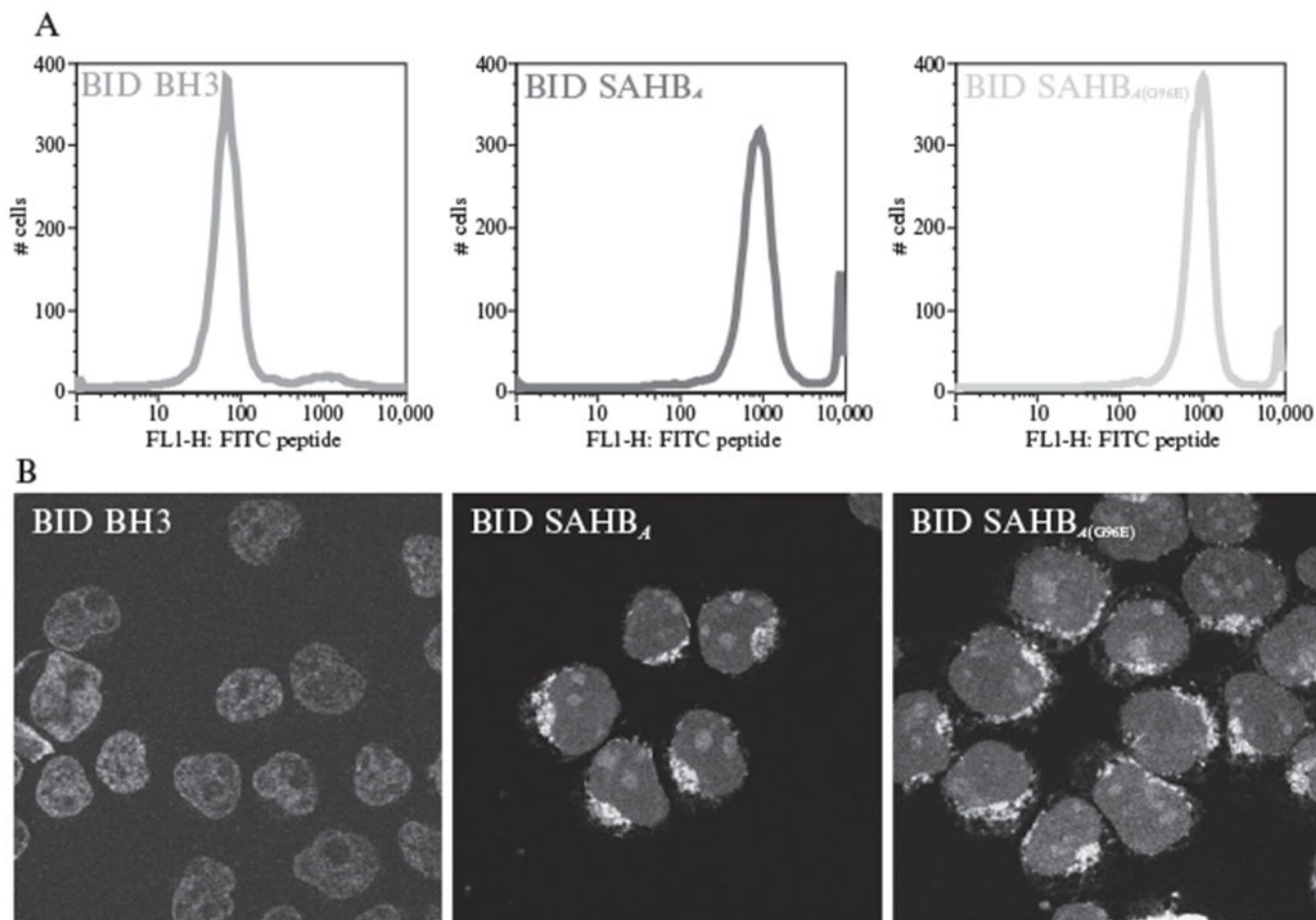


**Figure 22.7.** Cellular uptake of FITC-BID SAHB and a point mutant derivative, but not the unmodified FITC-BID BH3 peptide, is readily demonstrated by (A) FACS analysis and (B) confocal microscopy of FITC-peptide treated cells in culture. The cellular fluorescence of FITC-SAHB treated cells, as reflected by a shift of the FACS profile to the right compared to FITC-BID BH3-treated cells, corresponds to the intracellular cytosolic localization of FITC-BID SAHB observed by confocal microscopy. (Walensky et al., 2004)